Miniaturized Chipless RFID Tags Based on Periodically Loaded Microstrip Structure

Maha Added
Physical Department,
University of Tunis el Manar,
Tunis, Tunisia
maha.added@gmail.com

Karima Rabaani
Physical Department,
University of Tunis el Manar,
Tunis, Tunisia
rabaanikarmia@hotmail.fr

Safa Chabaan
Physical Department,
University of Tunis el Manar,
Tunis, Tunisia
safa.chebaane90@gmail.com

Noureddine Boulejfen
Research Center for Microelectronics and Nanotechnology,
Technopole of Sousse,
Sousse, Tunisia
nboulejf@ucalgary.ca

Abstract—**A compact chipless radio frequency identification (RFID) tag-based on slow-wave technology is introduced in this paper. The tag consists of a resonant circuit based on open stub resonators periodically loaded by shunt stubs allowing a coding capacity of 9 bits and operating in a frequency range from 2 to 4GHz. The receiving and transmitting antennas of the tag are particularly designed to minimize the tag size as much as possible. The proposed tag presents a robust bit pattern with a compact and fully printable structure using FR4 substrate for a low-cost tag.**

Keywords-chipless RFID tag; slow-wave technology; coding capacity

I. Introduction

Radio Frequency IDentification (RFID) is one of the most rapidly growing segments of modern automatic capture and identification. However, conventional chipped RFID systems have many limitations related to the use of the chip such as high cost, susceptibility in harsh environments, short life of the chip battery packs, etc. To overcome these limits, chipless RFID systems appear where the tag is a fully passive microwave structure and its encoding data depends only to its geometry [1]. Frequency domain chipless RFID tags use spectral signature to encode data [6]. Frequency domain tags are classified into two main families, the RCS-based tags and the retransmission-based tags. The RCS-based tags use resonant antennas that receive the signal and send it back with the tag signature [1-7]. Generally, they can reach a high coding capacity with a compact size. In [1], a compact RCS-based tag using resonant antennas in C form was proposed. The reported tag offers a coding capacity of 20 bits operating in a frequency range from 2 to 4GHz and with an overall size of 25×70mm². However, the RCS-based tags generally have a short reading range [2, 3] and a strong mutual coupling, which limits the data encoding capacity [4]. Concerning the retransmission-based tags [8-13], single or double antennas are used to receive and transmit the signal. The spectral signature of the tag is obtained by a resonant circuit with multiple resonators where each of them creates a notch or a peak around a given frequency point. The chipless tag introduced in [13] is a retransmission-based tag using spiral resonators that allow the coding of 35 bits in a frequency band ranging from 3.1 to 7GHz. Even if retransmission-based tags usually have an important size, this type of chipless tags has a robust bit pattern and ensures a large reading range compared to the RCS-based tags thanks to the use of independent antennas for both transmission and reception. In this paper, the miniaturization technique based on the slow wave approach has been used to design a 9-bit compact retransmission-based tag operating in a frequency band of 2 to 4GHz. For a complete chipless tag, dual cross-polarized monopole antennas were designed and connected to the resonant circuit to establish a communication link with the interrogator.

II. Tag Design

The retransmission-based tag presented in this paper consists of a resonant circuit of nine resonators connected to two cross polarized antennas, one for the transmission and the one for the reception. As it is shown in Figure 1, a basic chipless RFID tag structure can be composed of the known resonant circuit based on quarter-wave open stub resonators and two identical ordinary rectangular monopole antennas. The overall dimensions of the basic chipless RFID structure are around 119×73mm².

A. Resonant Circuit Design

1) Basic Resonant Circuit Structure

A basic structure of a resonant circuit can be based on the known quarter-wave open stub resonators as shown in Figure 2. This structure has been realized using the FR4 substrate with

Corresponding author: Maha Added

thickness h=0.4mm, dielectric constant ε_r=4.7 and loss tangent $tg\delta$=0.019. As presented in the Figure 2, the initial design of the prototype contains 9 open stub resonators equally spaced with 1mm apart to avoid mutual coupling. The length of each resonator is equal to $\lambda g/4$ at its corresponding resonant frequency, where λg is the wavelength in the substrate. The resonance frequency is independent from the width of the resonator [9, 16]. The parameters of each resonator in the basic multi-resonantor are given in Table I.

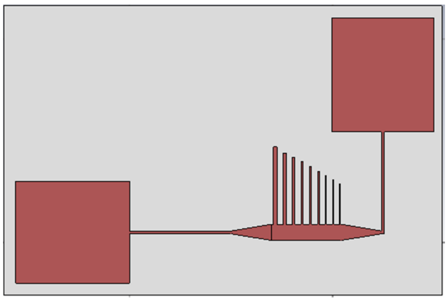

Fig. 1. Basic chipless RFID tag structure

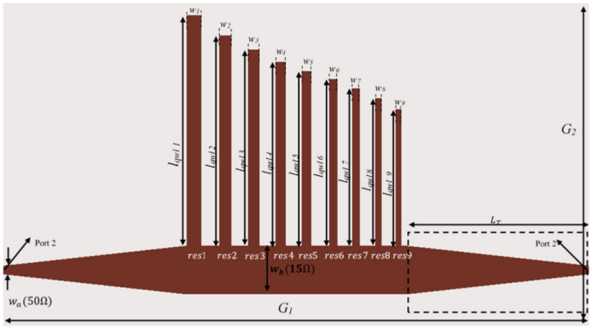

Fig. 2. Basic resonant circuit structure, G1=46 mm, G2=25 mm

A tuning process using Agilent ADS momentum software has revealed that high Q resonances can be obtained with a 15Ω feed line, such that w_b=4mm. Thus, a taper impedance transformer is required to match the input impedance of the resonant circuit to 50Ω. The length of the taper section is equal to $\lambda g/4$ with respect to the lowest operating frequency. In this work, the appropriate length of the impedance transformer section is found to be L_T=14.5mm. The resonant circuit response exhibits 9 resonance frequencies and thus a coding capacity of 9 bits, where the operating frequency range is between 2 and 4.5GHz. The overall dimensions of the obtained circuit are about 46×25mm².

2) Miniaturized Resonant Circuit Structure

Starting from the basic resonant circuit described above, a slow wave structure is used to reduce the size of the initial circuit while keeping the same electrical behavior. Periodically loading transmission lines with shunt capacitances can increase their effective electrical length [14]. Using this concept, significant size reduction of several passive microwave components have been achieved. For instance, the technology of periodically loaded slow wave microstrip lines has been used in [14] to miniaturize the size of branch-line and rate-race couplers and in [15] to design miniaturized single-band two-way and dual-band two-way Wilkinson power dividers. In this paper, slow-wave structure is developed for the miniaturization of chipless RFID tags. Based on the slow-wave concept, a conventional microstrip line with a given length is substituted for a shorter microstrip line loaded with equally spaced capacitances terminated to ground. The role of the loading capacitances is to slow down the wave propagation within the microstrip line. This results in a longer effective electrical length compared to an unloaded microstrip line. Based on this approach one can accurately determine the values of the loading capacitances C_p and their spacing d to guarantee the desired electrical behavior while reducing the line length. Let's consider an unloaded lossless transmission line with characteristic impedance Z_{c_un} and a phase velocity V_{p_un} given by [15] such as:

$$Z_{c\_un} = \sqrt{\frac{L}{C}} \qquad (1)$$

$$V_{p\_un} = \frac{1}{\sqrt{LC}} \qquad (2)$$

where L and C are the line inductance and capacitance of the transmission line respectively.

Loading periodically the transmission line with equally spaced shunt capacitors C_p allows the reduction of its effective characteristic impedance Z_{c_lo} and phase velocity V_{p_lo}. For a spacing d between the capacitors less than the signal wavelength, Z_{c_lo} and V_{p_lo} are given by [15] as:

$$Z_{c\_lo} = \sqrt{\frac{L}{C+\frac{C_p}{d}}} \qquad (3)$$

$$V_{p\_lo} = \frac{1}{\sqrt{L\,(C+\frac{C_p}{d})}} \qquad (4)$$

Equation (4) shows the reduction of the phase velocity V_{p_lo} compared to that of the unloaded line. This means that an effective electrical length can be achieved using a transmission line with a shorter physical length. The effective electrical length of the loaded line is expressed as:

$$\Phi_{lo} = \frac{N d \omega_0}{V_{p\_lo}} = N d \omega_0 \sqrt{L\left(C + \frac{C_p}{d}\right)} \qquad (5)$$

where N is the number of the loading capacitors and ω_0 is the angular frequency of interest. Using (1)-(5) we can determine the value of C_p and the spacing d of the loading capacitors:

$$d = \frac{Z_{c\_lo}\Phi_{lo}\ V_{p\_un}}{N\,\omega_0 Z_{c\_un}} \qquad (6)$$

$$C_p = \frac{\Phi_{lo}(Z_{c\_un}{}^2 - Z_{c\_lo}{}^2)}{N\,\omega_0 Z_{c\_un}{}^2 Z_{c\_lo}} \qquad (7)$$

To obtain an entirely planar circuit, the loading capacitances C_p can be realized using open-circuit stubs by applying the following formula [15]:

$$C_p = \frac{l_{stub}}{Z_{c\_stub} V_{p\_stub}} \text{ for } \frac{\omega_0}{V_{p\_stub}} l_{stub} \ll 1 \qquad (8)$$

where l_{stub}, Z_{c_stub} and V_{p_stub} are the length, characteristic impedance and phase velocity of the stub respectively.

3) Design Considerations

To achieve the highest possible reduction, the impedance of the unloaded line Z_{c_un} should be at its highest possible value which is obtained by choosing the lowest possible microstrip width that can be manufactured. In addition, to minimize the crosstalk between stubs, the spacing d must be greater than $3h$ where h is the height of the substrate. This condition ($d \geq 3h$) can be relaxed by placing the stubs on both sides of the line. Taking into account these design considerations, the resulting slow wave structure can be duplicated for all the resonators of the proposed resonant circuit. Depending on the frequency of resonance of each resonator a corresponding stub length is required. As previously mentioned, to obtain the highest possible line length reduction (l/l_{qwl}), the characteristic impedance of the unloaded microstrip line Z_{c_un} should be at its highest value, so its width should be at the lowest possible value. In this work, the width of all the unloaded microstrip lines is fixed to w_{un}=0.2mm allowing a characteristic impedance of 94Ω. For a planar structure, the capacitances C_p implemented using open stubs with a similar width for all the resonators and length that varies from one resonator to the other as described by (8). To avoid mutual coupling between the stubs, the spacing d is fixed to 0.6mm for all resonators and stubs are alternatively placed on both sides of the line as shown in Figure 3. The number of sections N is chosen to be the same for all the resonators. Consequently, different resonance frequencies can be obtained by changing the stub length l_{stub}.

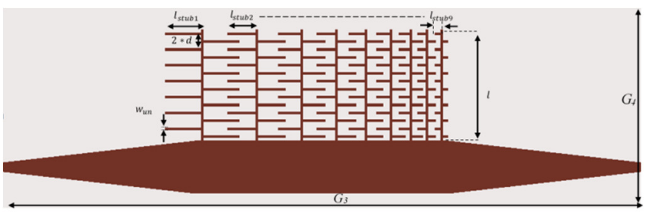

Fig. 3. Slow wave resonant circuit, G3=46mm, G4=14mm

Table I illustrates the resonance frequencies, the parameters of each quarter-wave resonator with the capacitance and stub length of its corresponding slow-wave structure. Knowing that d=0.6mm and N=14, the length of the unloaded stub for all the resonators is $l=N \times d$=8.4mm. Figure 3 shows the slow wave structure based resonant circuit. The spacing between resonators is fixed such as to avoid the coupling effect and to ensure the stability of the resonance frequencies when changing the configuration pattern of the resonant circuit. The dimensions of the slow wave structure based resonant circuit are 48×14mm² offering a size reduction of 41.6% compared to the basic resonant circuit. To validate the obtained values of C_p and l_{stub}, the simulation of both circuits is performed without considering the coupling effect using Agilent ADS simulator. The comparison between the transmission responses of the basic quarter-wave length based resonant circuit and the slow wave structure based one is illustrated in Figure 4, which shows a good match between the two responses, which validates the calculated values and the slow-wave structure efficiency with a size reduction of 41.6% while keeping the same coding capacity and operating frequency range. The simulated and measured transmission responses of the proposed slow wave based resonant circuit in the presence of coupling effects are discussed in Section III.

TABLE I. PHYSICAL AND ELECTRICAL PARAMETERS OF THE SLOW WAVE BASED RESONATORS VS QUARTER-WAVELENGTH RESONATORS

		Quarter-wavelength resonator			Slow wave resonator		
Res.	**Freq. (GHz)**	l_{qwl} **(mm)**	w **(mm)**	Z_{c_qwl} **(Ω)**	C_p **(pF)**	l_{stub} **(mm)**	**Length reduction (%)**
res1	2.28	18.9	1.16	39.7	0.257	2.8	55.5
res2	2.52	17.23	1	43.8	0.201	2.2	51.2
res3	2.72	16.08	0.88	47.4	0.164	1.8	47.7
res4	2.919	15.05	0.789	50.6	0.137	1.5	44.2
res5	3.07	14.3	0.724	53.2	0.118	1.3	41.6
res6	3.25	13.64	0.654	56.3	0.1	1.1	38.5
res7	3.459	12.9	0.583	60	0.08	0.9	34.9
res8	3.716	12.07	0.507	64.4	0.063	0.7	30.4
res9	4.045	11.18	0.426	70.1	0.045	0.5	24.9

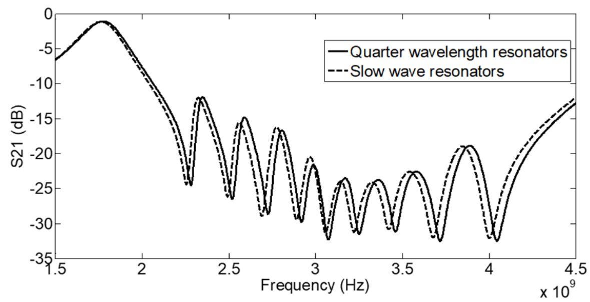

Fig. 4. Comparison between the transmission responses of quarter-wave resonant circuit and based slow wave resonant circuit without considering the coupling effect

B. Antenna Designs

Omni-directional monopole UWB antennas are generally used for signal reception and transmission in chipless tags (Figure 1). These antennas are known by their relatively big size, which further increases the overall size of the tag.

1) Receiving Antenna

For a miniaturized antenna structure, an omni-directional monopole UWB antenna with a slow wave feed line has been designed. The structure of the proposed antenna using the slow wave based feed line is presented in Figure 5. The addition of slots in the ground plane is required to improve the reflection response of the antenna. The positions, forms, and dimensions of the slots are chosen according to the surface current density in the antenna. The dimensions of the antenna have been reduced to 26×44mm². The simulated and measured responses of the proposed antenna are presented and discussed below.

2) Transmitting Antenna

The transmission antenna of the tag is designed in a way to minimize as much as possible the size of the tag while keeping its horizontal polarization to avoid cross talk between transmitted and received signals. Therefore, as shown in Figure 6, a rectangular monopole UWB antenna with a bended feed line is used. The bending of the feed line allowed a good space management of the entire tag. However, it resulted in a ground plane shape modification leading to performance degradation. To overcome this problem some feed line length tuning has been performed. Figure 6 shows the final shape and the design parameters of the transmitting antenna.

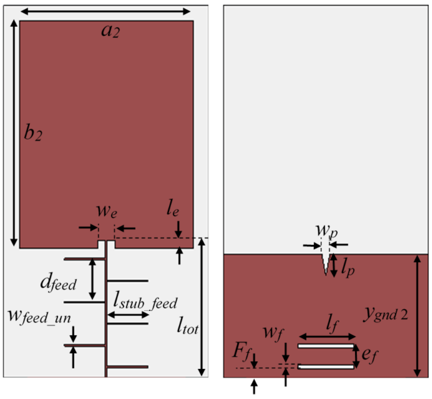

Fig. 5. Structure of receiving antenna based on slow wave feed line: y_{gnd2}=14.54mm, l_p=2.5mm, w_p=1mm, l_f=7mm, w_f=0.5mm, e_f=2mm, F_f=1mm, w_e=2.2mm,;l_e=1mm, b_2=27mm, a_2=22mm

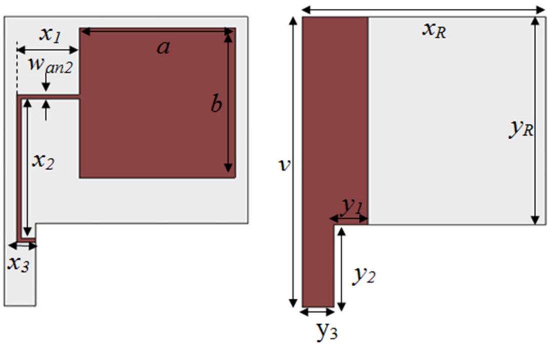

Fig. 6. Transmitting antenna structure: x_R=39mm, y_R=36mm, y_1=5.5mm, $y2$=14.25mm, y_3=5mm, y_4=50.25mm, x_1=10mm, x_2=24.25mm, x_3=2.4mm, w_{an2}=0.7mm

Figure 7 presents the new tag structure using the designed antennas. The size of the whole tag is about 66.5×55mm² allowing a miniaturization of 58.2% compared to the basic structure tag described in Figure 1. To study the mutual coupling effect between antennas and to fix the spacing threshold between the two radiating elements, each antenna is excited by a plane wave and simulated independently in the presence of the other antenna.

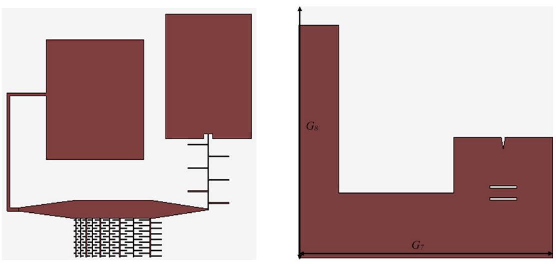

Fig. 7. Final chipless RFID tag structure: G_7=66.5mm, G_8=55mm

III. Results and Discussion

So far, to build up a clearer picture of the real behavior of the resonant circuit, an electromagnetic simulation that considers the coupling effects is required. Therefore, a simulation using CST Studio Suit has been performed for different tag codes. For the experimental validation of the proposed miniaturization approach, the developed resonant circuit has been fabricated in the all-one configuration as shown in Figure 8(a). Then its transmission coefficient has been measured in the 1.5-5GHz frequency band. Figure 8(b) shows a good agreement between the measured and the CST-simulated (with coupling) transmission coefficients.

(a)

(b)

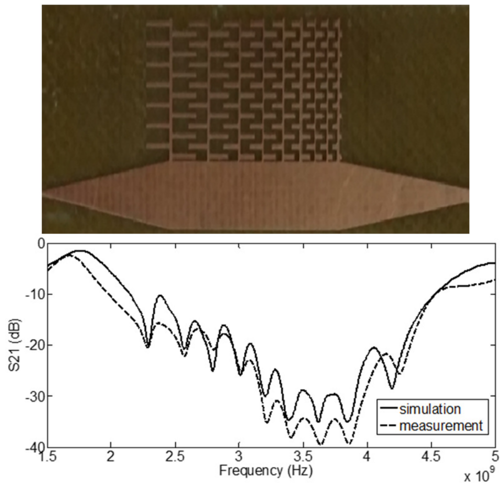

Fig. 8. Slow wave based resonant circuit: (a) realized resonant circuit, (b) simulated and measured responses

Each resonator branch of the resonant circuit operates at a correspondent frequency allowing a coding capacity of 9 bits. When all the resonators are connected to the main transmission line the resulting tag code is set to 111111111 and the resonance frequencies are: 2.28GHz, 2.58GHz, 2.8GHz, 3GHz, 3.22GHz, 3.41GHz, 3.63GHz, 3.85GHz, and 4.26GHz. Each bit in the code is set or reset by connecting or disconnecting the corresponding resonator branch from the main transmission line. As presented in Figure 9, *res2*, *res4*, *res6* and *res8* are disconnected from the transmission line to set the tag code to 101010101. After the preliminary validation using the all-one realized resonant circuit, a comparison between the simulated and measured results has been performed for the resonant circuit with the tag code set to 101010101. As revealed by Figure 10 a good agreement between the measured and the simulated results has been observed.

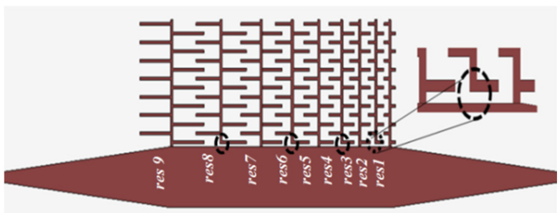

Fig. 9. Chipless RFID tag configuration with tag code set to 101010101

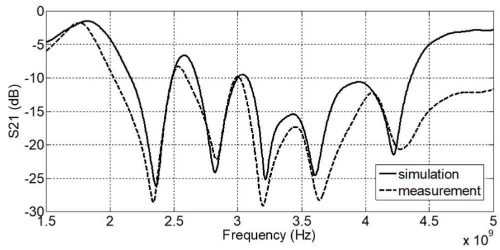

Fig. 10. Simulated and measured transmission responses of the resonant circuit with tag code set to 101010101

As a next stage, a comparison between two different measured tag codes has been performed. Figure 11 includes the measured transmission responses of resonant circuits with tag codes set to 111111111 and 101010101. The figure shows clearly that the resonance frequencies are quite stable even if the tag code changes, which demonstrates the coding robustness of the proposed resonant circuit.

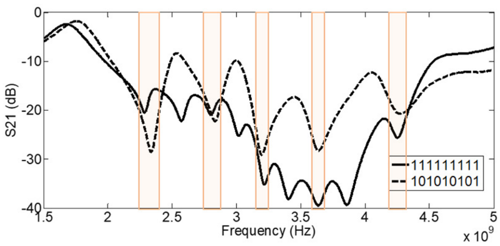

Fig. 11. Measured transmission responses of resonant circuits with tag codes set to 111111111 and 101010101

For experimental validation purposes, the designed slow wave based antenna has been fabricated and measured over the 1.5 to 5GHz frequency band. The fabricated antenna is presented in Figure 12(a) while Figure 12(b) illustrates the simulated and the measured reflection coefficients. According to the measured reflection coefficient illustrated in Figure 12(b), the proposed antenna is well matched between 1.6GHz and 4.5GHz, which covers the operating frequency band of the proposed resonant circuit. Furthermore, the radiation efficiency, the radiation pattern and the gain of the proposed antenna have been simulated. As it is shown in Figure 13(a), the radiation efficiency of the antenna is around 70% for the entire operating frequency band. The simulated radiation pattern of the antenna, illustrated in Figure 13(b), is omnidirectional with a gain around 2.2dBi which confirms that the designed antenna is suitable for RFID applications.

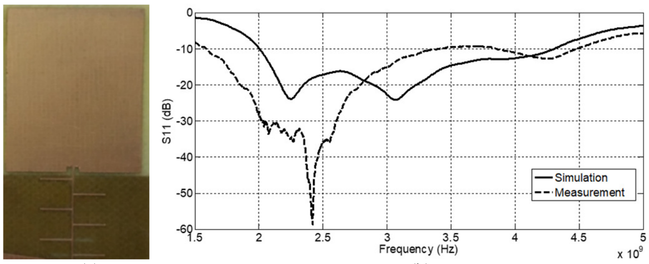

(a) (b)

Fig. 12. (a) Realized receiving antenna, (b) simulated and measured reflection coefficient

(a)

(b)

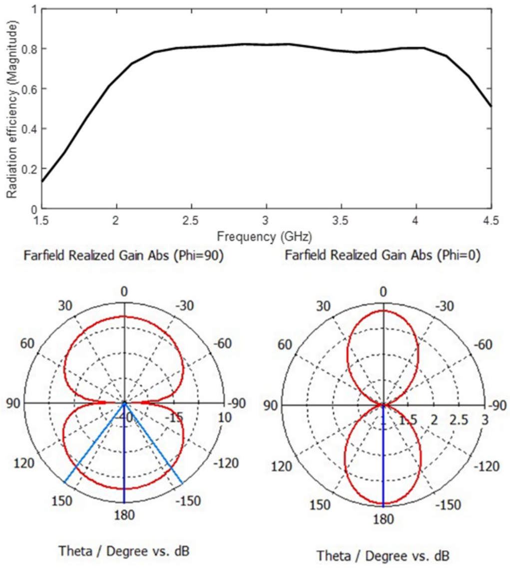

Fig. 13. Radiation efficiency and radiation pattern of the slow wave based antenna: (a) Radiation efficiency, (b) the radiation pattern at H and E plane respectively

Regarding the transmitting antenna described in Figure 6, the corresponding simulated and measured reflection coefficients are illustrated in Figure 14(b) showing that the operating bandwidth of the antenna is between 2.2GHz and 4.3GHz which is also adequate to the frequency range of the multi resonant circuit. The radiation pattern of the antenna presented in Figure 15 is almost omnidirectional and the gain in the operating frequency range is about 2.2dBi, which confirms that the designed antenna is suitable for RFID applications. Table III presents a comparison between different RFID chipless retransmission-based tags including this work.

(a)

(b)

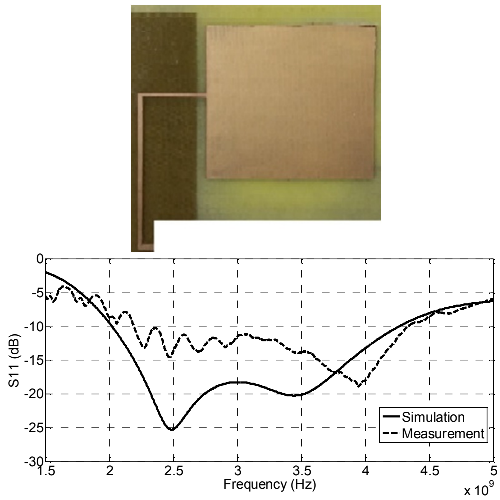

Fig. 14. Transmitting antenna: (a) Realized transmitting antenna, (b) comparison of simulated and measured reflexion response of the transmitting antenna

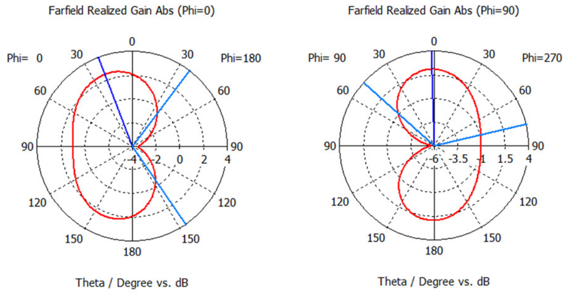

(a) (b)

Fig. 15. Radiation pattern of the transmitting antenna: (a) H-plane, (b) E-plane

TABLE II. COMPARISON BETWEEN DIFFERENT CHIPLESS TAGS

Ref.	Used approach	Coding capacity	Frequency range (GHz)	Size
[9]	Triangle microstrip filter	6 bits	4-7	150×30mm² (without antennas)
[10]	Microstrip open resonators	8 bits	2-4	80×60mm² (with antenna)
[12]	SIW	1 bit	10.5-11	10×10mm² (without antennas)
This work	Slow wave resonator	9 bits	2-4	66×55mm² (with antennas)

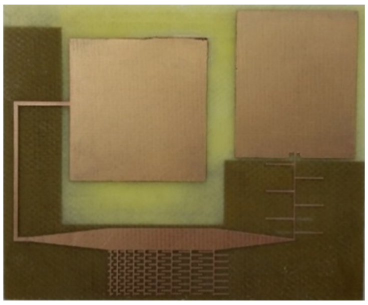

Fig. 16. The realized proposed chipless RFID tag

IV. CONCLUSION

In this paper, a slow-wave structure was used to miniaturize a RFID chipless retransmission-based tag. Firstly, a slow-wave structure based multi-resonator has been developed and a size reduction of 41.6% was reached compared to the quarter-wave open stub resonators. The developed multi resonator includes nine open stub resonators periodically loaded by shunt stubs. The resonance frequency of each resonator depends only on the length of its shunt stubs. The nine resulting resonance frequencies lay in the 2.28 to 4.26GHz range. Simulation results not included in this paper revealed that with the use of the Roger 4003C substrate instead of the FR4 one can further reduce the size of the nine bit multi-resonator and improve its behavior. Therefore, a miniaturized rectangular monopole UWB antenna, which is used as the receiving antenna of the tag, has been designed using a slow-wave structure, while respecting the required operating frequency range and allowing omnidirectional pattern. With a good space management of the whole tag, a reduction of more than 58% has been obtained compared to the basic tag structure which demonstrated the efficiency of the used approach for designing miniaturized chipless RFID tags.

REFERENCES

[1] A. Vena, E. Perret, S. Tadjini, "A fully printable chipless RFID tag with detuning correction technique", IEEE Microwave and Wireless Components Letters, Vol. 22, No. 4, pp. 209-211, 2012

[2] M. A. Islam, N. C. Karmakar, "A novel compact printable dual-polarized chipless RFID system", IEEE Transactions on Microwave Theory and Techniques, Vol. 60, No. 7, pp. 2142-2151, 2012

[3] H. S. Jang, W. G. Lim, K. S. Oh, S. M. Moon, J. W. Yu, "Design of low-cost chipless system using printable chipless tag with electromagnetic code", IEEE Microwave and Wireless Components Letters, Vol. 20, No. 11, pp. 640-642, 2010

[4] I. Jalaly, I. D. Robertson, "Capacitively-Tuned Split Microstrip Resonators for RFID Barcodes", European Microwave Conference, Paris, France, October 4-6, 2005

[5] M. Martinez , D. V. D. Weid, "Compact Slot-Based Chipless RFID Tag", IEEE RFID Technology and Application Conference, Tampere, Finland, September 8-9, 2014

[6] M. S. Bhuiyan, N. Karmakar, "Chipless RFID Tag Based on Split-Wheel Resonators", 7th European Conference on Antennas and Propagation, Gothenburg, Sweden, April 8-12, 2013

[7] C. M. Nijas, U. Deepak, P. V. Vinesh, R. Sujith, S. Mridula, K. Vasudevan, P. Mohanan, "Low-cost multiple-bit encoded chipless RFID tag using stepped impedance resonator", IEEE Transactions on Antennas and Propagation, Vol. 62, No. 9, pp. 4762-4770, 2014

[8] C. S. Hartmann, "A Global SAW ID Tag with Large Data Capacity", IEEE Ultrasonics Symposium, Munich, Germany, October 8-11, 2002

[9] C. M. Nijas, R. Dinesh, U. Deepak, A. Rasheed, S. Mirdula, K. Vasudevan, P. Mohanan, "Chipless RFID tag using multiple microstrip open stub resonators", IEEE Transactions on Antennas and Propagation, Vol. 60, No. 9, pp. 4429-4432, 2012

[10] M. E. Jalil, M. K. A. Rahim, N. A. Samsuri, R. Dewan, "Chipless RFID Tag Based on Meandered Line Resonator", IEEE Asia-Pacific Conference on Applied Electromagnetics, Johor Bahru, Malaysia, December 8-10, 2014

[11] H. E. Matbouly, N. Boubekeur, F. Domingue, "A novel chipless identification tag based on a substrate integrated cavity resonator", IEEE Microwave and Wireless Components Letters, Vol. 23, No. 1, pp. 52-54, 2013

[12] S. Moscato, R. Moro, M. Bozzi, L. Perregrini, S. Sakouhi, F. Dhawadi, A. Gharsallah, P. Savazzi, A. Vizziello, P. Gamba, "Chipless RFID for Space Applications", IEEE International Conference on Wireless for Space and Extreme Environments, Noordwijk, Netherlands, October 30-31, 2014

[13] S. Preradovic, N. C. Karmakar, "Design of Fully Printable Planar Chipless RFID Transponder with 35-Bit Data Capacity", European Microwave Conference, Rome, Italy, September 29-October 1, 2009

[14] K. W. Eccleston, S. H. M. Ong, "Compact planar microstripline branch-line and rat-race couplers", IEEE Transactions on Microwave Theory and Techniques, Vol. 51, No. 1, pp. 2119-2125, 2003

[15] J. S. Hong, M. J. Lancaster, "Capacitively loaded microstrip loop resonator", Electronics Letters, Vol. 30, No. 18, pp. 1494-1495, 1994

[16] K. Rawat, F. M. Ghannouchi, "A design methodology for miniaturized power dividers using periodically loaded slow wave structure with dual-band applications", IEEE Transactions on Microwave Theory and Techniques, Vol. 57, No. 12, pp. 3380-3388, 2009

[17] C. Zhou, H. Y. D. Yang, "Design considerations of miniaturized least dispersive periodic slow-wave structures", IEEE Transactions on Microwave Theory and Techniques, Vol. 56, No. 2, pp. 467-474, 2008